Science and Technology Indonesia
e-ISSN:2580-4391 *p*-ISSN:2580-4405
Vol. 11, No. 1, January 2026

Research Paper

Optimization and Stability Assessment of Chitosan/PVA Smart Sensor Films Incorporated with Roselle Anthocyanins for Real-Time Visual Monitoring of Chicken and Shrimp Freshness under Different Storage Conditions

Alfianita Nuril Hidayaty[1], Saidun Fiddaroini[1], Ahmad Luthfi Fahmi[1], Qonitah Fardiyah[1], Akhmad Sabarudin[1,2*]

[1]*Department of Chemistry, Faculty of Sciences, Universitas Brawijaya, Malang, 65145, Indonesia*
[2]*Research Center for Advanced System and Material Technology, Brawijaya University, Malang, 65145, Indonesia*
***Corresponding author**: sabarjpn@ub.ac.id*

Abstract
The development of intelligent packaging systems has become a promising approach to ensure food safety and quality by enabling real-time freshness monitoring. In this study, chitosan/polyvinyl alcohol (Cs/PVA)-based smart sensor films incorporated with roselle (*Hibiscus sabdariffa* L.) anthocyanins were fabricated and optimized for the visual detection of chicken and shrimp spoilage under variations storage. Anthocyanins were extracted from fresh roselle petals through different maceration periods (R1–R5) to investigate their influence on film properties. Physicochemical characterization revealed that extended maceration enhanced anthocyanin loading, leading to increased film thickness, higher color saturation, and improved optical responsiveness. FESEM micrographs demonstrated homogeneous polymer matrices at lower anthocyanin concentrations, while higher loadings induced micro-aggregates that enhanced volatile adsorption and sensing sensitivity. The fabricated films exhibited clear and progressive color transitions aligned with the spoilage process: red–purple at fresh conditions (pH 5–6), brown–green at intermediate spoilage (pH 7–9), and yellow–brown at advanced spoilage (pH ≥10), consistent with anthocyanin structural transformations. Storage trials with chicken and shrimp confirmed that the Cs/PVA–R5 film displayed the intense coloration and strong response to volatile amines such as ammonia, trimethylamine, and dimethylamine, enabling reliable freshness monitoring. Importantly, the films provided a visual indication when the pH exceeded the edibility threshold of 7.0–7.5, beyond which the samples were deemed unsuitable for consumption. Overall, this work demonstrates the potential of Cs/PVA–roselle anthocyanin films as eco-friendly, low-cost, and effective smart indicators for meat and seafood freshness, offering a practical platform for intelligent food packaging applications.

Keywords
Chitosan, Polyvinyl Alcohol, Roselle Anthocyanin, Smart Film, Colorimetric Sensor, Meat Freshness

Received: 30 August 2025, Accepted: 21 November 2025
https://doi.org/10.26554/sti.2026.11.1.217-234

1. INTRODUCTION

Food is a fundamental element of human life, and ensuring access to safe and high-quality food is recognized as a basic human right. However, fresh or minimally processed products are highly prone to quality deterioration caused by physical, chemical, and microbiological processes (Karanth et al., 2023; Mafe et al., 2024). Among these, chicken and shrimp represents one of the most widely consumed fresh foods but is classified as a highly perishable commodity due to its rapid spoilage. This short shelf-life results from its high water and protein content, which accelerates microbial proliferation and enzymatic degradation, leading to a rapid decline in sensory and nutritional quality if not properly handled (Genç et al., 2025; Katiyo et al., 2020). Inadequate handling also increases the risk of bacterial contamination, while endogenous enzymatic reactions and microbial colonization further compromise freshness and safety (Augustyńska-Prejsnar et al., 2024; Klaharn et al., 2022).

To safeguard quality and ensure food safety, continuous freshness assessment throughout the supply chain is essential. Among various metrics, the total volatile base nitrogen (TVB-N) value remains one of the most reliable indicators for evaluating fish spoilage. TVB-N primarily comprises ammonia (NH_3), trimethylamine (TMA), and dimethylamine (DMA), which are generated from the enzymatic degradation of trimethylamine oxide (TMAO) during spoilage (Zhai et al., 2017). Monitoring TVB-N thus provides a quantitative framework for assessing fish freshness and forms the scientific basis for developing rapid, non-destructive freshness sensors.

To meet the growing demand for sustainable, real-time

food-quality monitoring, colorimetric freshness indicators have emerged as an attractive approach. Anthocyanins natural pigments from plants such as roselle. offer pH-responsive chromatic transitions from red to blue or yellow as their flavylium cations transform into quinoidal bases or chalcones under alkaline conditions (Erna et al., 2022). Their color and stability are strongly influenced by factors such as pH, oxygen, light, temperature, and molecular structure, making them highly suitable for pH-sensitive food products (Rosalina et al., 2022). Chitosan is a biodegradable and biocompatible natural polysaccharide derived from crustacean shells, composed of β-(1 → 4)-linked D-glucosamine and N-acetyl-D-glucosamine units (Kusumawati et al., 2025). Embedding anthocyanins within biodegradable biopolymer matrices such as chitosan/polyvinyl alcohol (Cs–PVA) produces eco-friendly, compatibility, non-destructive sensors capable of reporting freshness without direct contact with food (Amaregouda and Kamanna, 2023; Ma et al., 2024; Zhang et al., 2019). Yet, optimizing pigment loading, film thickness, and dispersion remains critical for achieving both high sensitivity and mechanical stability.

Conventional freshness evaluation methods, including sensory inspection, microbial plate counts, and chemical assays such as TVB-N, are often labor-intensive, destructive, and time-consuming, thereby limiting their application for continuous monitoring across supply chains (Low et al., 2022; Sigurðardóttir et al., 2025). Moreover, these approaches typically require trained personnel and laboratory equipment, which constrains their deployment in real-world retail and household contexts. As a result, there is growing interest in developing simple, non-invasive systems capable of detecting spoilage volatiles or pH changes in situ, thereby offering rapid and reliable freshness information without damaging the product.

Within this context, intelligent packaging and colorimetric indicator labels incorporating natural pigments have emerged as promising solutions for real-time freshness monitoring. Anthocyanin-based films respond to the alkaline volatile bases generated during spoilage, particularly ammonia and biogenic amines, by undergoing visually distinct color transitions correlated with product quality (Sinela et al., 2017). However, achieving optimal performance requires careful tuning of pigment concentration, polymer composition, and microstructure to balance sensitivity, mechanical integrity, and pigment stability.

The distinction between this study and previous works is considerable. Zhai et al. (2017) developed colorimetric films using a starch/PVA matrix, whereas Zhang et al. (2019) produced indicators based on starch/PVA and chitosan/PVA composites enriched with roselle anthocyanins, applying them solely to pork stored at 25 °C. Latiff et al. (2025), in contrast, employed gelatin as the primary polymer. Building upon these foundations, the present work adopts a chitosan–polyvinyl alcohol hybrid matrix integrated with roselle anthocyanin extract obtained through controlled maceration (1–5 days), enabling fine modulation of pigment loading and pH sensitivity. The films are further assessed for real-time freshness monitoring of both chicken and shrimp under three practical storage conditions ambient (23 °C), refrigeration (6 °C), and freezing (–10 °C) providing a wider evaluation range than prior single-temperature or single-product studies.

Recent advances indicate that chitosan–PVA composites offer a biodegradable, transparent, and mechanically stable platform capable of enhancing anthocyanin stability and strengthening chromogenic responsiveness. Leveraging these advantages, this study presents an optimized Cs/PVA-based indicator film that demonstrates improved pigment retention, structural integrity, and functional compatibility relative to starch- or gelatin-based systems. The formulation is supported by comprehensive characterization, including FTIR, FESEM, LC–HR-MS, stereo-microscopy, and statistical validation (ANOVA), alongside a three-month color-stability assessment. Together, these elements establish a robust innovation framework that extends beyond descriptive colorimetric reporting and positions the work as a meaningful advancement in intelligent food-freshness sensing.

To address the growing need for sustainable, intelligent sensors, this work reports the development of a biodegradable colorimetric film integrating roselle-derived anthocyanins within a chitosan–polyvinyl alcohol (Cs–PVA) matrix, offering tunable sensitivity toward ammonia vapor. The film enables real-time, non-destructive freshness monitoring of chicken and shrimp through pronounced, pH-responsive color shifts under both ambient and refrigerated conditions. Chromogenic responses were quantified via smartphone-assisted RGB analysis and converted into an easy-to-interpret, instrument-free indicator card for end-user applications. Comprehensive UV–Vis, FTIR, and FESEM analyses elucidated the structural, chemical, and functional attributes of the films, while CIELAB and RGB measurements confirmed consistent responsiveness across pH 3–12 and 1% ammonia exposure. Subsequent freshness trials validated the system's practical performance, establishing it as a reliable, eco-friendly, and scalable platform for smart food-quality monitoring and supply-chain assurance with minimal environmental impact.

2. EXPERIMENTAL SECTION

2.1 Materials and Instrumentation

All chemicals and solvents employed in this study were of analytical grade and used without any further purification. Ultrapure water (resistivity ≥18.2 MΩ · cm) and 75% (v/v) ethanol served as extraction media for isolating anthocyanins from fresh roselle (*Hibiscus sabdariffa* L.), which was utilized as the natural pigment source.

Buffers and analytical reagents were prepared as follows: potassium dihydrogen phosphate (KH_2PO_4, 0.02 M; Sigma-Aldrich, >99.0%), citric acid monohydrate ($C_6H_8O_7{\cdot}H_2O$, 0.02 M; Sigma-Aldrich, >98%), disodium hydrogen phosphate (Na_2HPO_4, 0.02 M; Emsure), sodium bicarbonate ($NaHCO_3$, 0.02 M; Sigma-Aldrich, 99.5–100.5%), sodium hydroxide (NaOH, 0.02 M; Emsure), and sodium carbonate (Na_2CO_3, 0.02 M;

© 2026 The Authors.

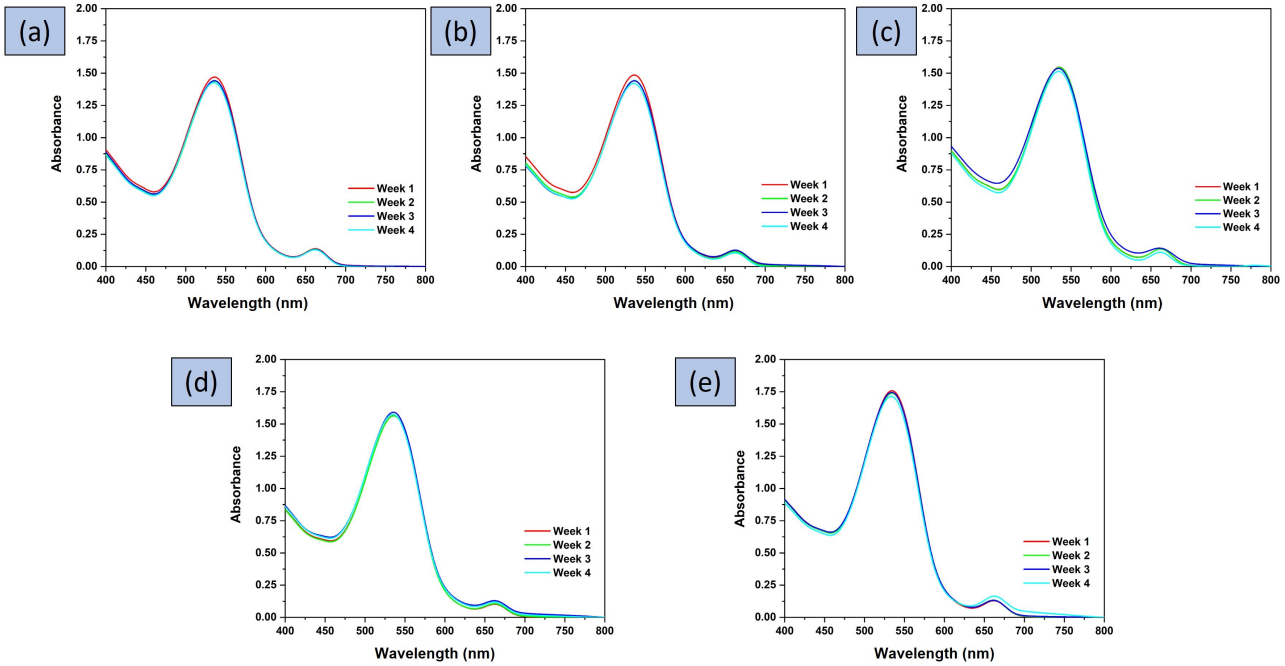

Figure 1. Stability Profile of Fresh Roselle Flower Extract Under Different Maceration Durations: (a) 1 Day, (b) 2 Days, (c) 3 Days, (d) 4 Days, and (e) 5 Days

Sigma-Aldrich, >99.0%). Additional materials included potassium chloride (KCl; Sigma-Aldrich), sodium acetate (3.28 g; Sigma-Aldrich), and glacial acetic acid (98%; EMSURE).

For film preparation, low–molecular-weight chitosan (Sigma-Aldrich; degree of deacetylation 75–85%) was dissolved in 2% (v/v) aqueous glacial acetic acid, while polyvinyl alcohol (PVA, 5% w/v; Emsure) was dissolved in deionized water. These components were combined to produce chitosan/PVA–anthocyanin composite films intended for colorimetric applications to assess the freshness of chicken (*Gallus gallus domesticus*) and shrimp (*Litopenaeus vannamei*). Analytical characterization was conducted using a UV–Vis spectrophotometer (Shimadzu UV-1600 series), a Fourier-transform infrared (FTIR) spectrometer (Shimadzu 8400s), and a field emission scanning electron microscope (FESEM; FEI Quanta FEG 650) in Integrated Research Laboratory, Brawijaya University.

2.2 Extraction and Characterization of Roselle Flowers

2.2.1 Extraction of Anthocyanins from Fresh Roselle Flowers

Fresh roselle flowers were first blended and then manually ground with a mortar and pestle to reduce particle size. The homogenized plant material was mixed with 75% (v/v) ethanol at a solid-to-solvent ratio of 1:10 (w/v) (Abdelghany et al., 2019). Maceration was carried out at ambient temperature for 1, 2, 3, 4, and 5 days to evaluate the effect of extraction time. Following maceration, the mixture was clarified by centrifugation at 3,000 rpm for 20 min. The supernatant was subsequently filtered through Whatman filter paper to obtain a clear extract. The filtrate was concentrated using a rotary evaporator (40 °C) to remove ethanol. The resulting anthocyanin-rich extract was transferred into amber sample vials and stored at 4 °C until further analysis.

2.2.2 Storage and Stability Monitoring Prior to Solvent Removal

Following centrifugation and filtration, the roselle anthocyanin extract was stored at 4 ± 1 °C for up to 1 month before rotary evaporation. The stability of the extract during refrigerated storage was monitored weekly by recording UV–Vis absorption spectra (200–800 nm) using a Shimadzu UV–Vis spectrophotometer (UV-1600 series) (Zhang et al., 2026).

2.2.3 Determination of Total Anthocyanin Content

The anthocyanin concentration in the roselle extract was determined using the pH differential method combined with UV–Visible spectrophotometry. Two buffer systems were prepared for pH calibration: (i) 0.025 M potassium chloride (KCl, 0.186 g; Sigma-Aldrich) adjusted to pH 1.0 using 37% hydrochloric acid, and (ii) 0.4 M sodium acetate (3.28 g; Sigma-Aldrich) adjusted to pH 4.5 with glacial acetic acid. The pH values of both buffers were verified using a calibrated pH meter.

For sample preparation, 1 mL of the extract was diluted with 9 mL of 0.025 M KCl buffer (pH 1.0) to obtain the acidic solution, while another 1 mL of the extract was mixed with 9 mL of 0.4 M sodium acetate buffer (pH 4.5) to produce

© 2026 The Authors.

the reference solution. Both solutions were analyzed using a UV–Vis spectrophotometer at the anthocyanin maximum absorption wavelength (λmax), with an additional wavelength applied to correct for turbidity. The absorbance value (A) was determined according to Equation 1:

$$A = \left[(A(\lambda_{max}) - A(\lambda_{correction}))_{pH\ 1.0}\right] - \left[(A(\lambda_{max}) - A(\lambda_{correction}))_{pH\ 4.5}\right] \quad (1)$$

The total anthocyanin concentration (TAC), expressed in mg/L, was determined using the following Equation 2:

$$\text{TAC (mg/L)} = \frac{A \times MW \times DF \times 1000}{\varepsilon \times L} \quad (2)$$

The total anthocyanin content is determined using several parameters. The absorbance difference (A) is measured between the sample solutions at pH 1.0 and pH 4.5. The molecular weight (MW) of the predominant anthocyanin, generally cyanidin-3-glucoside, is considered, with a value of 449.2 g/-mol. A dilution factor (DF) is applied when the sample undergoes dilution prior to measurement. The calculation also incorporates the molar extinction coefficient (ϵ) of cyanidin-3-glucoside, which is 26,900 L·mol^{-1}·cm^{-1} at its maximum absorbance wavelength of 520 nm (Zhai et al., 2017). Lastly, the optical path length of the cuvette (L), typically 1 cm, is included to account for the distance the light travels through the sample during absorbance measurement.

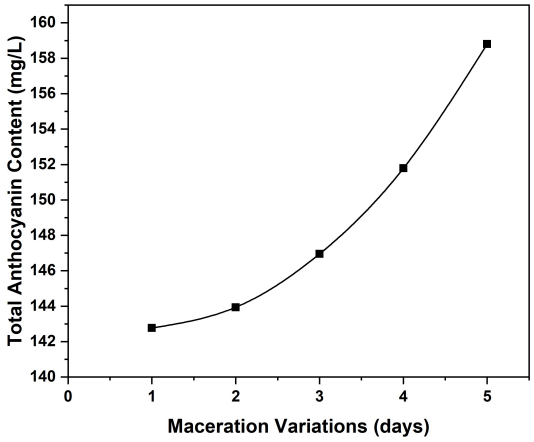

Figure 2. Total Anthocyanin Content of Roselle Extracts Obtained from Different Maceration Periods

2.2.4 UV–Vis Spectroscopic Analysis of Roselle Anthocyanin Extract

The roselle anthocyanin extract was analyzed using UV–Visible spectrophotometry within the 400–800 nm range to examine its absorbance profile across the visible spectrum. Measurements were conducted under varying pH conditions (pH 3–12)

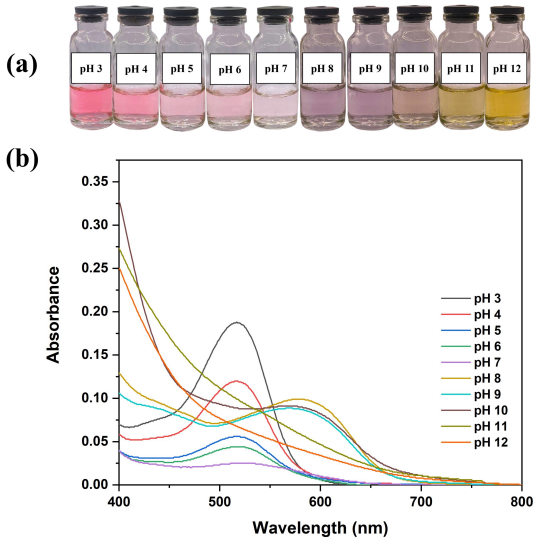

Figure 3. Color Variation (a) and UV–Visible Absorption Spectra (b) of Roselle Extract Across Different pH Conditions (pH 3–12)

to assess both spectral properties and associated color changes. For each analysis, 100 μL of extract was combined with 5 mL of 0.02 M buffer solution adjusted to the corresponding pH. The wavelength of maximum absorption (λmax) at each pH level was determined from the recorded spectra, with special emphasis on bathochromic and hypsochromic shifts that reflect structural modifications of the anthocyanin chromophores (Zhai et al., 2017).

2.3 Formulation of Chitosan–PVA–Roselle Anthocyanin-Based Colorimetric Films

Prior to use, chitosan and polyvinyl alcohol (PVA) powders were pre-dried in a vacuum oven at 60 °C for 1 h to remove residual moisture and enhance solubility. The chitosan solution was prepared by dissolving 2.0 g of chitosan in 100 mL of distilled water containing 2% (v/v) glacial acetic acid, followed by magnetic stirring at 75 °C for 1 h. Separately, 5.0 g of PVA was dissolved in 100 mL of distilled water under continuous stirring at 90 °C and then cooled to ambient temperature (Xu et al., 2023).

Equal portions of the two polymer solutions 10 mL of chitosan solution and 10 mL of PVA solution (1:1 v/v) were then combined to produce the chitosan/PVA (Cs/PVA) base matrix, which served as the polymeric foundation for subsequent incorporation of roselle anthocyanin extracts. Roselle anthocyanin extract was incorporated into the Cs/PVA blend at five concentration levels (equivalent to extracts from 1–5 days of maceration per 20 mL polymer mixture), yielding formulations designated Cs/PVA-R1 through Cs/PVA-R5. Each mixture was homogenized by continuous stirring for 2 h to promote uniform pigment dispersion and stable interactions within the polymer matrix.

© 2026 The Authors.

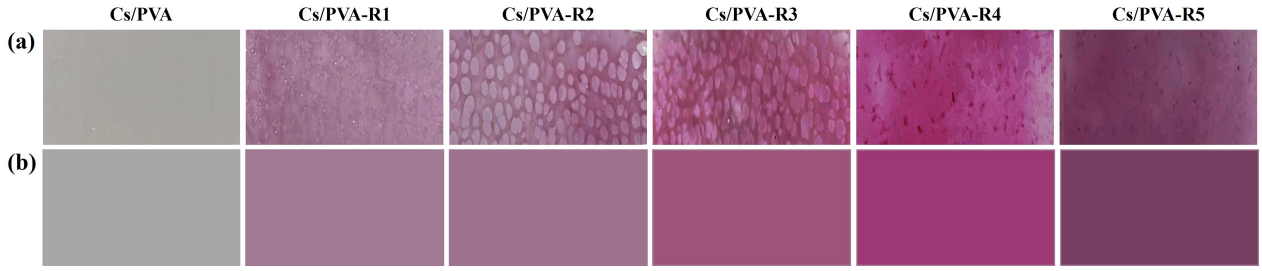

Figure 4. Visual Appearance of the Samples (a) and Corresponding RGB Intensity Profiles Derived from ImageJ Analysis (b)

Subsequently, 20 mL of each formulation was cast into sterile 90 mm glass Petri dishes, leveled to eliminate air bubbles, and dried under vacuum at 40 °C for 24 h (Vevor laboratory incubator) to minimize oxidation and pigment degradation. After drying, the films were gently detached and photographed using an iPhone 13 under controlled lighting conditions. RGB color data were extracted and analyzed using ImageJ software by selecting uniform regions and processing histograms to establish a reference for subsequent colorimetric response evaluations. The resulting films were sealed individually in polyethylene pouches and stored at −10 ± 1°C in the dark to preserve anthocyanin stability prior to physicochemical characterization and functional performance testing.

2.4 Characterization of Colorimetric Films

2.4.1 Fourier Transform Infrared (FTIR) Spectroscopy

Characterization of the colorimetric films commenced with sample preparation, followed by Fourier Transform Infrared (FTIR) analysis using a spectrometer equipped with OMNIC software. Spectra were acquired at room temperature in absorbance mode over the 4000–500 cm^{-1} range, with a resolution of 4 cm^{-1} and 32 co-added scans per sample (Fiddaroini et al., 2025). The OMNIC software package was utilized to process and interpret the spectra, enabling the identification of characteristic functional groups and chemical bonds present in the films. This analysis provided insights into possible molecular interactions among chitosan, polyvinyl alcohol (PVA), and the anthocyanin compounds incorporated into the composite matrix.

2.4.2 Field Emission Scanning Electron Microscopy (FE-SEM)

Colorimetric films were initially prepared and sputter-coated with a thin layer of gold to enhance surface conductivity and improve imaging quality. The coated samples were mounted onto specimen holders and examined using a JEOL JSM-6360 LV Field Emission Scanning Electron Microscope (FESEM). Instrumental settings such as magnification, focus, and beam alignment were carefully optimized prior to image acquisition, with the analysis conducted at an accelerating voltage of 20 kV (Fiddaroini et al., 2025).

2.4.3 Thickness Measurement

The thickness of the colorimetric films was measured using a high-precision digital micrometer (measurement range 0–10 mm; accuracy ±0.001 mm). Ten measurements were taken at randomly selected points across each sample, encompassing both central and peripheral regions to account for possible thickness variability (Zhai et al., 2017). Each formulation (Cs/PVA-R1 through Cs/PVA-R5) was analyzed in triplicate to ensure reproducibility and data accuracy. Mean thickness values and corresponding standard deviations were calculated to assess the effect of anthocyanin concentration on film uniformity and structural consistency.

2.5 Quantitative Evaluation of Colorimetric Film Response to Ammonia Vapor

To evaluate ammonia responsiveness, rectangular film strips (1 × 5 cm) were secured to the inner surfaces of sterile Petri dish lids, while the bases of the dishes contained 20 mL of 1% (w/v) NH_4OH solution. The Petri dishes were tightly sealed and maintained at 23 ± 1 °C for 4 h. Color changes of the films were documented at 30-minute intervals over a total exposure period of 180 minutes using an iPhone 13 under standardized lighting conditions within a Puluz lightbox.

Captured images were analyzed using ImageJ software, where RGB (Red, Green, and Blue) intensity values were extracted from calibrated regions of interest. The corresponding changes in the red, green, and blue channels were calculated using Equations (3)–(5), respectively. The films' response to ammonia vapors was quantified using a colorimetric sensitivity index (SRGB) according to Equation 6:

$$\Delta R = |R_a - R_b| \tag{3}$$

$$\Delta G = |G_a - G_b| \tag{4}$$

$$\Delta B = |B_a - B_b| \tag{5}$$

$$S_{RGB} = \frac{\Delta R + \Delta G + \Delta B}{R_a + G_a + B_a} \times 100 \tag{6}$$

Higher S_{RGB} values denote greater reactivity of the film to ammonia, indicating better suitability for freshness indicator applications (Zhang et al., 2026).

© 2026 The Authors.

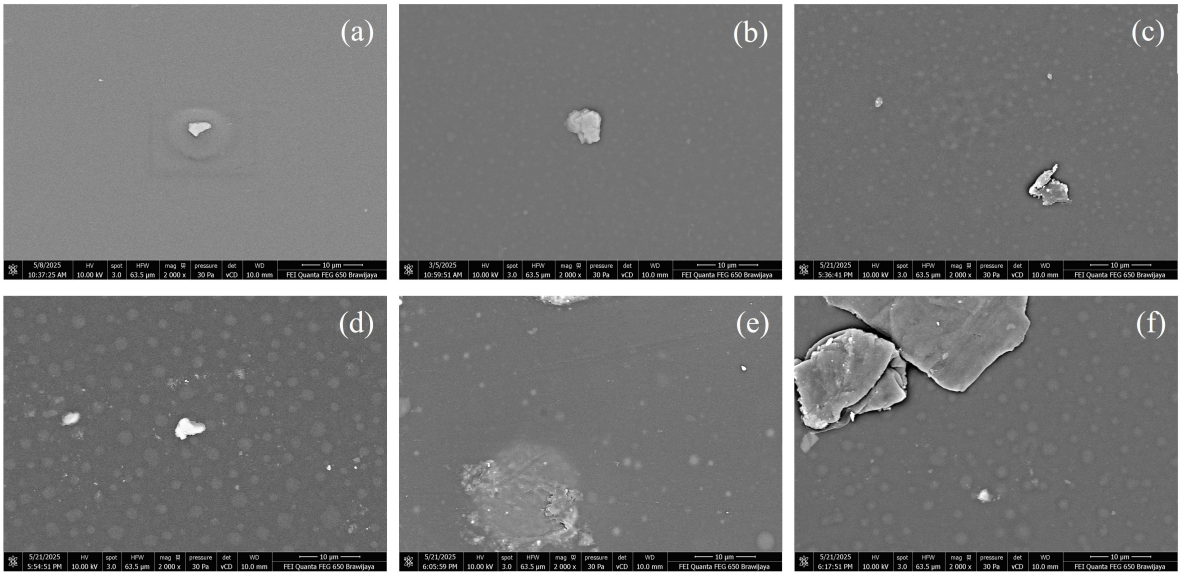

Figure 5. FESEM Micrographs Captured at 250× Magnification Showing (a) Cs/PVA, (b) Cs/PVA-R1, (c) Cs/PVA-R2, (d) Cs/PVA-R3, (e) Cs/PVA-R4, and (f) Cs/PVA-R5

2.6 Determination of Colorimetric Film Properties and pH Response

The pH responsiveness of the chitosan/PVA–roselle anthocyanin films was evaluated by immersing each formulation (Cs/PVA-R1 through Cs/PVA-R5) in 0.02 M phosphate buffer solutions adjusted to pH 3.0–12.0. Samples were maintained under static conditions at 23 ± 1 °C for 10 min to ensure uniform interaction between the polymer matrix and the buffer medium. After immersion, the films' visual appearance was recorded using a high-resolution digital camera under standardized illumination and a neutral white background to minimize optical artifacts. Quantitative color measurements were subsequently obtained using a smartphone-based colorimeter application (developed by Serhii Smyk), which provided CIELAB coordinates (Equations 7-9): L* (lightness), a* (red–green axis), and b* (yellow–blue axis). Three separate regions were analyzed on each film surface, and mean values were calculated (Chen et al., 2021).

$$\Delta L^* = L^*_{\text{sample}} - L^*_{\text{standard}} \quad (7)$$

$$\Delta a^* = a^*_{\text{sample}} - a^*_{\text{standard}} \quad (8)$$

$$\Delta b^* = b^*_{\text{sample}} - b^*_{\text{standard}} \quad (9)$$

The total color difference (ΔE) under each pH condition was determined according to Equation 10:

$$\Delta E = \sqrt{\Delta L^2 + \Delta a^2 + \Delta b^2} \quad (10)$$

The baseline CIELAB values of the control Cs/PVA film were used as reference coordinates. The resulting ΔE values quantitatively represented the chromatic shift and pH sensitivity of the films across the tested range.

2.7 Potential Uses of Colorimetric Films in Monitoring Shrimp and Chicken Freshness

To evaluate the practical performance of the developed colorimetric indicators, a simulation study was conducted using approximately 25 g of chicken (*Gallus gallus domesticus*) and 25 g of shrimp (*Litopenaeus vannamei*). Each sample was placed in a sterile Petri dish, and a 1 × 5 cm Cs/PVA-R5 film strip was affixed to the inner surface of the lid to enable non-contact interaction with the headspace volatiles generated during spoilage. The experiment encompassed three storage conditions: ambient temperature (23 ± 1 °C) with color variations recorded every 6 h for 24 h, refrigerated storage at 6 °C with daily monitoring for up to 10 days, and frozen storage at −10 °C with weekly observations extended to 13 weeks. Colorimetric changes were quantified by calculating the total color difference (ΔE) in the CIELAB color coordinate system, which served as the principal parameter for assessing both indicator responsiveness and spoilage progression in the test samples (Zhao et al., 2022).

3. RESULT AND DISCUSSIONS

3.1 Characterization of Roselle Extract

3.1.1 Stability of Roselle Extract During Storage

Figure 1 shows that roselle anthocyanin extracts obtained from different maceration periods (1–5 days) and stored at 4 °C remained relatively stable over a four-week period. All samples retained their main absorption band at approximately 500–550

© 2026 The Authors.

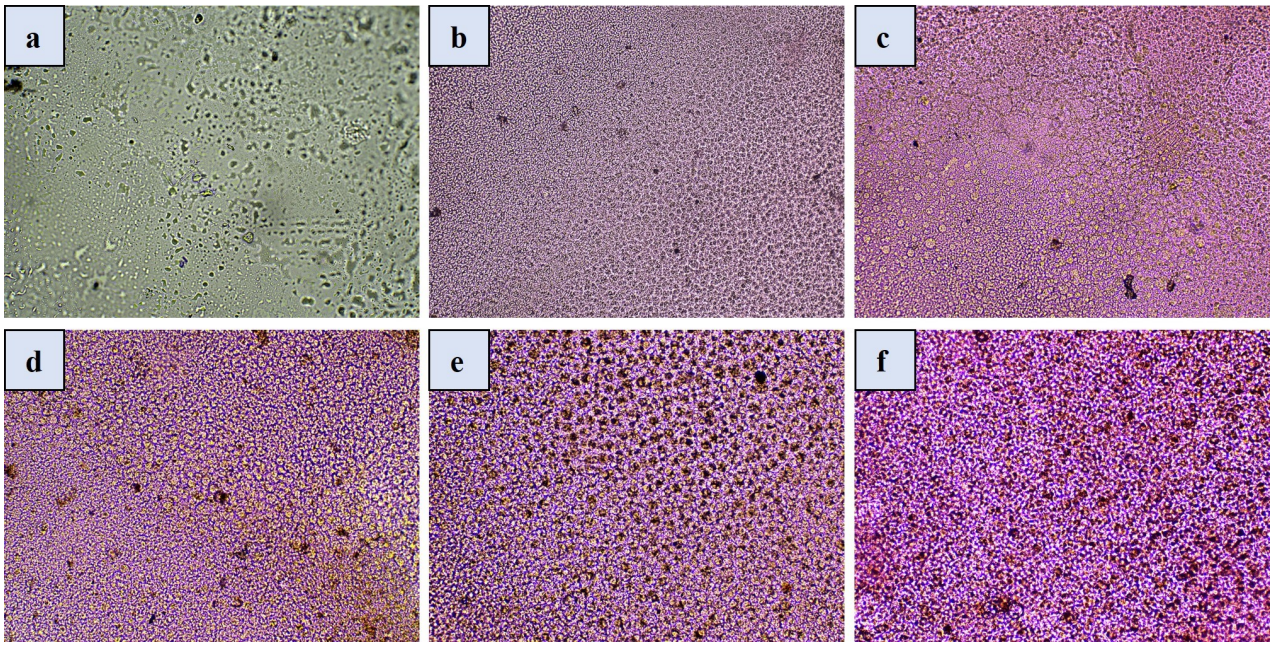

Figure 6. Stereo Microscopic Images of (a) Cs/PVA, (b) Cs/PVA-R1, (c) Cs/PVA-R2, (d) Cs/PVA-R3, (e) Cs/PVA-R4, and (f) Cs/PVA-R5

nm without any significant shifts in λmax, indicating that the core pigment structure remained intact. A slight decrease in absorbance intensity was observed with increasing storage time, particularly for extracts derived from longer maceration periods (4–5 days), suggesting partial degradation, likely due to oxidation or the formation of less stable species such as chalcones and anthocyanin polymers. Nevertheless, the decline was minimal, indicating that the storage conditions (refrigeration at 4 °C and darkness prior to evaporation) were effective in preserving pigment stability.

These findings are consistent with previous reports showing that roselle anthocyanins exhibit relatively high stability under cold storage. Previous study state that roselle extract stored at 4 °C for 60 days showed only moderate degradation (Sinela et al., 2017). Likewise, broader literature confirms that key factors affecting anthocyanin stability include temperature, pH, oxygen, light, and pigment concentration (Enaru et al., 2021).

3.1.2 Determination of Total Anthocyanin Content

The total anthocyanin content (TAC) of roselle extracts increased systematically with maceration time, ranging from 142.77 mg/L on day 1 to 158.80 mg/L on day 5 (Figure 2). This upward trend reflects the higher extraction yield of anthocyanins from roselle. with prolonged maceration, which enhances pigment release and solubilization in the ethanolic medium (Lai et al., 2024). Longer maceration increases the interaction between the solvent and plant tissue, promoting cell-wall disruption and diffusion of anthocyanin molecules, thereby enriching the total pigment concentration within the film matrix (Mawarno et al., 2024).

This increase in TAC over the 1–5 day maceration range is significant for the performance of the colorimetric indicators. Anthocyanin concentration directly affects the optical density, color intensity, and pH responsiveness of the films (Mawarno et al., 2024). Higher pigment loading, as observed in the five-day maceration extract, generally produces stronger color contrast and faster response kinetics toward volatile bases such as ammonia due to an increased number of active chromophoric sites and stronger hydrogen-bonding/electrostatic

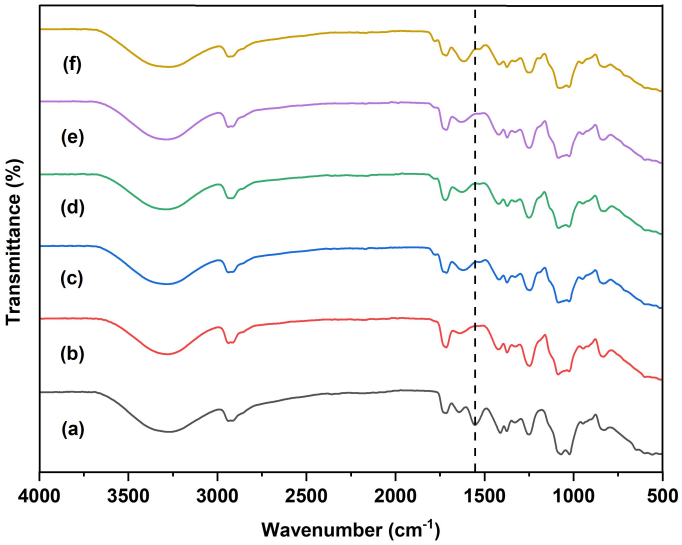

Figure 7. FTIR Spectra of Cs/PVA-R Composite Films, Illustrating (a) Cs/PVA, (b) Cs/PVA-R1, (c) Cs/PVA-R2, (d) Cs/PVA-R3, (e) Cs/PVA-R4, and (f) Cs/PVA-R5

© 2026 The Authors.

Table 1. Visual Color Response of Cs/PVA-R Films to 1% Ammonia Vapor Exposure

Time (min)	Cs/PVA	Cs/PVA-R1	Cs/PVA-R2	Cs/PVA-R3	Cs/PVA-R4	Cs/PVA-R5
1						
30						
60						
90						
120						
150						
180						
210						
240						

interactions with the Cs/PVA matrix. However, excessively high pigment concentrations can also promote pigment aggregation and reduce homogeneity, potentially affecting film transparency and mechanical integrity (Gomes et al., 2024).

The TAC values observed in this study are also consistent with previous reports on roselle anthocyanins, which typically range from 140 to 160 mg/L under optimized extraction conditions (Suzery et al., 2020). This consistency highlights the importance of carefully adjusting extraction and formulation parameters to achieve the desired sensitivity and performance for freshness monitoring applications.

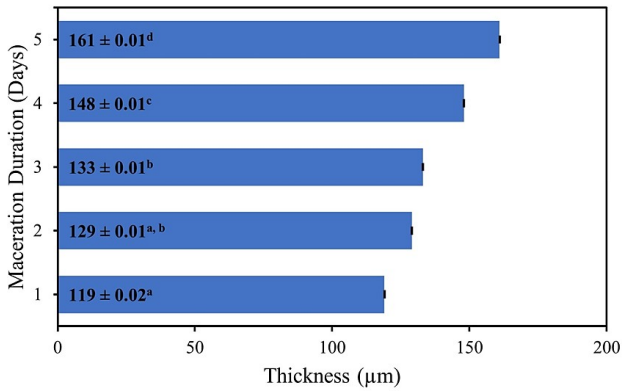

Figure 8. Thickness Measurements (n=3) of Cs/PVA-Based Films Incorporating Varying Maceration Levels of Roselle Extract (R 1–5)

3.1.3 UV–Vis Spectral Properties of Roselle Anthocyanins under Varying pH Conditions

Figure 3 shows the strong pH-dependent chromatic and spectroscopic behavior of the roselle anthocyanin extract. As presented in panel Figure 3a, the extract appears bright red under acidic conditions (pH 3–4), turns pink to violet near neutral pH (5–7), and shifts to brownish-yellow at alkaline pH (9–12). These visible changes correspond to the transformation of anthocyanins from flavylium cations to quinoidal bases and ultimately chalcone or hemiketal forms as the medium becomes more basic.

Figure 3b confirms these observations: at low pH, a distinct absorption band is centered near 520 nm, which gradually decreases in intensity and broadens with increasing pH, while at higher pH the absorption peak shifts or disappears entirely. This behavior indicates progressive deprotonation and structural rearrangement of the anthocyanin chromophores, which is consistent with previous findings on roselle anthocyanin extract (Castañeda-Ovando et al., 2009).

3.2 Characterization of Colorimetric Films

3.2.1 Optical and Colorimetric Properties of Films with Various Anthocyanin Extract

The visual (Figure 4a) and digital colorimetric (Figure 4b) data together provide a coherent and mechanistic account of how maceration-driven increases in anthocyanin loading modulate the optical and functional properties of Cs/PVA films. Visually, films prepared from progressively longer maceration extracts (R1 → R5) exhibit a systematic deepening of hue from pale pink to intense purplish-red; quantitative RGB-to-CIELab analysis performed in ImageJ corroborates this observation, showing a monotonic increase in the a* (redness) coordinate accompanied by a concomitant decrease in L* (lightness). This trend is entirely consistent with the expected hyperchromic and bathochromic behaviour of anthocyanin chromophores as their solution and solid-phase concentration increases: higher chromophore density amplifies light absorption at visible λmax values, producing greater perceived saturation and lower reflected light intensity in the films. Roselle anthocyanin extract studies showing improved pigment yield and chromatic intensity with extended extraction times (Sinela et al., 2017).

From a materials-chemistry perspective, the measured colour progression and the spatial uniformity of RGB/CIELab values indicate two important attributes of the composite system. First, extended maceration increases the total anthocyanin content available for incorporation, a consequence of enhanced

© 2026 The Authors.

solvent penetration and progressive liberation of vacuolar pigments from the plant matrix; by the Beer–Lambert relation, this higher loading produces proportionally greater absorbance and, therefore, stronger colour signals in the dry film. Second, the observed homogeneity of RGB values across selected regions implies effective miscibility and molecular-level dispersion of anthocyanins within the Cs/PVA host. Mechanistically, this compatibility likely arises from extensive hydrogen-bonding and electrostatic interactions between anthocyanin hydroxyl/flavylium functionalities and the polar groups of chitosan ($-NH_2$/$-NH_3^+$) and PVA (–OH), which both stabilise the pigments against phase separation and immobilise them within the polymer network (see also evidence for homogeneous pigment dispersion in polymer matrices (Du et al., 2021).

Overall, the combination of visual inspection and digital color analysis confirms that the fabricated films possess stable and tunable color properties, suitable for subsequent pH or volatile-sensing applications in smart sensor systems.

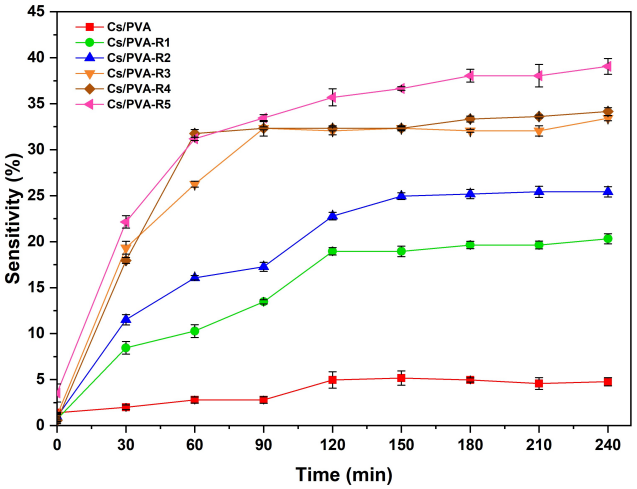

Figure 9. Colorimetric Film Sensitivity (%) Under Exposure to 1% Ammonia at Different Maceration Periods (1–5 Days) n=3

3.2.2 Surface Morphological Analysis Using FESEM

The FESEM micrographs provide direct structural evidence of how roselle anthocyanin incorporation modulates the surface morphology of Cs/PVA films. The pristine Cs/PVA matrix (Figure 5a) displayed a smooth, compact, and continuous surface with no observable cracks or particulate domains, confirming the good miscibility and compatibility of chitosan and PVA chains, in line with prior reports on polysaccharide–polyol systems (Wang et al., 2017). Upon anthocyanin loading (R1–R5, Figure 5b–f), distinct morphological changes were observed, most notably the emergence of granular agglomerates and irregular surface features. These features are consistent with strong noncovalent interactions among anthocyanin molecules, primarily hydrogen bonding between hydroxyl/flavylium groups and π–π stacking between aromatic moieties, which favour self-

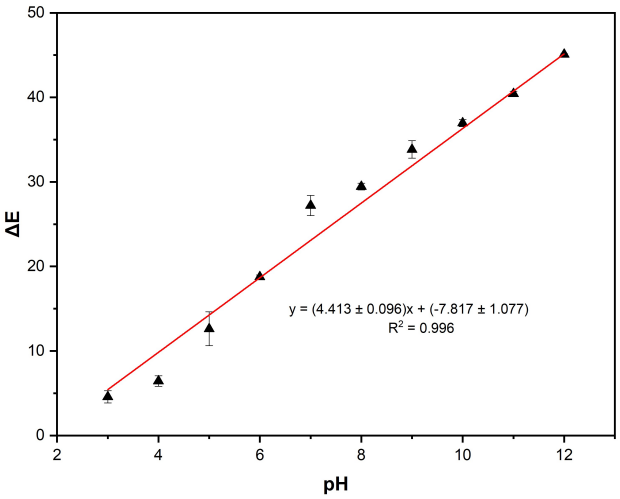

Figure 10. Statistical Analysis of the ΔE–pH Relationship for the Cs/PVA–R5 Film

association into supramolecular clusters rather than complete dispersion within the polymer network.

This partial aggregation has dual implications for material functionality. On one hand, the reduced homogeneity compromises the uniformity of the polymer matrix, which could lead to localised mechanical weaknesses and heterogeneity in optical transparency. On the other hand, the formation of microdomains increases surface roughness and potentially generates porous regions, which can enhance volatile molecule adsorption and thereby amplify the colorimetric response, particularly to alkaline gases such as ammonia. Such trade-offs between homogeneity and functional enhancement have been consistently observed in natural pigment–polysaccharide systems, where low pigment concentrations favour smooth and uniform films, while higher loadings induce aggregation and surface roughening (Abdelghany et al., 2019).

Collectively, these results underscore the pivotal role of pigment concentration and dispersion in dictating the balance between structural integrity and sensing performance of Cs/PVA–anthocyanin films. While achieving optimal homogeneity is crucial for maintaining consistent mechanical and barrier properties, a controlled degree of anthocyanin aggregation may be strategically advantageous, as it introduces textural heterogeneity that increases reactive surface area and enhances responsiveness in colorimetric sensing platforms.

3.2.3 Stereo Microscopic Observation of Chitosan/PVA–Roselle Anthocyanin Films

Stereo microscopic observation (Figure 6) revealed clear morphological transformations of the chitosan/polyvinyl alcohol (Cs/PVA) films as a function of anthocyanin extract incorporation and maceration duration. The pristine Cs/PVA film exhibited a relatively smooth, uniform, and translucent surface, indicating good miscibility and molecular compatibility

© 2026 The Authors.

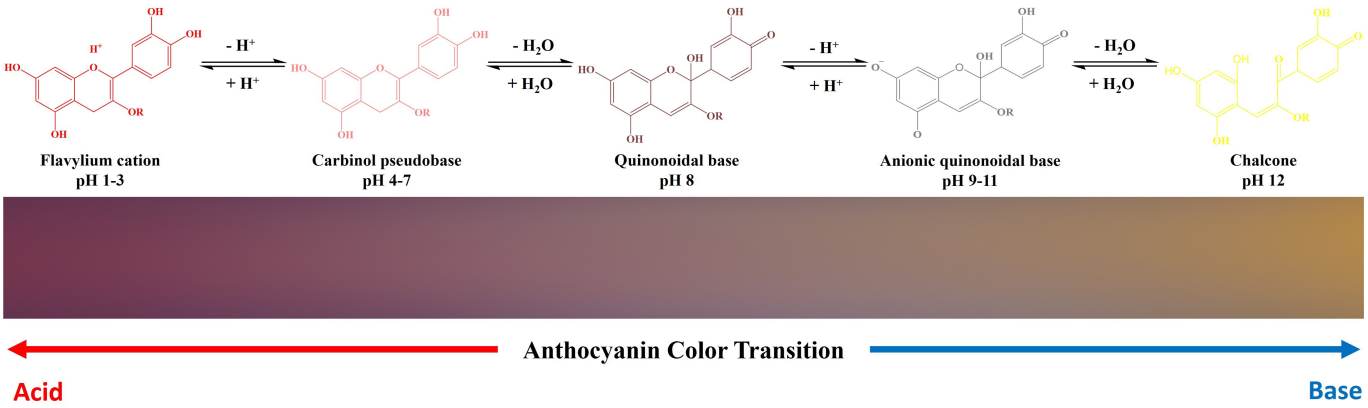

Figure 11. pH-Responsive Chromic Transition Mechanism of the Cs/PVA–R5 Film

between the chitosan and PVA chains. The faint bluish hue observed in the pristine film corresponds to the intrinsic intermolecular hydrogen-bonding interactions (–NH···O and –OH···O) between chitosan and PVA, which establish a stable polymeric network with high structural homogeneity (Bi et al., 2020; Merlusca et al., 2018; Zhang et al., 2024).

Upon anthocyanin incorporation (Cs/PVA–R1 to Cs/PVA–R5), the surface gradually evolved from uniform and faintly colored to increasingly textured with heterogeneous purple-red coloration. These color transitions, from bluish-violet (R1) to deep purple-red (R5), reflect the progressive loading and uniform dispersion of roselle anthocyanins within the polymeric matrix. The intensified chromatic response with longer maceration times indicates a higher pigment concentration and stronger interactions between the anthocyanin hydroxyl/flavylium groups and the amino or hydroxyl moieties of the Cs/PVA backbone. Such interactions occur primarily through hydrogen bonding and electrostatic attraction, resulting in the formation of stable polymer–pigment complexes that immobilize the anthocyanin molecules within the three-dimensional polymer network (Zheng et al., 2024).

The three-dimensional morphology observed under stereo microscopy shows that the Cs/PVA framework, represented by bluish regions, forms an interconnected matrix of polymer chains that physically entraps the anthocyanin molecules. The purple to reddish domains correspond to anthocyanin-rich zones embedded within the polymeric microstructure, indicating efficient pigment encapsulation without surface crystallization or phase separation. This morphology suggests that the anthocyanins are well integrated within the polymer matrix rather than merely adsorbed on the surface, which is critical for ensuring long-term stability, uniform color response, and resistance to leaching during application.

Notably, no microbial colonies or bacterial growth were detected across any of the film samples, confirming that the chitosan/PVA–roselle composite possesses intrinsic antibacterial characteristics. This antibacterial property can be attributed to the synergistic effects of chitosan's polycationic nature, which disrupts bacterial cell membranes via electrostatic interactions, and the phenolic constituents of roselle extract, which further inhibit microbial proliferation. The absence of bacterial contamination throughout the matrix surface and within its microstructure underscores the films' potential for food packaging applications where both freshness indication and antimicrobial protection are desirable.

Overall, the stereo microscopy analysis provides a comprehensive visualization of the structural and compositional integrity of the Cs/PVA–roselle anthocyanin films. The coexistence of the bluish polymeric network (chitosan–PVA matrix) and the purple-red anthocyanin domains demonstrates a well-organized three-dimensional hybrid structure, where the strong intermolecular hydrogen bonding between polymer chains and pigment molecules ensures mechanical robustness, optical homogeneity, and excellent antimicrobial stability essential features for smart, eco-friendly freshness indicator films.

3.2.4 Functional Group Identification Using FTIR Spectroscopy

Figure 7 presents the FTIR spectra of the neat Cs/PVA film (a) and Cs/PVA composite films containing roselle anthocyanin extracts (R1–R5) (b–f). The neat Cs/PVA film displayed characteristic absorption bands of chitosan and PVA: a broad band around 3300–3350 cm^{-1} corresponding to O–H and N–H stretching vibrations, peaks at 2920–2940 cm^{-1} attributed to C–H stretching of aliphatic groups, and bands at 1650–1600 cm^{-1} related to amide I (C=O stretching) and amide II (N–H bending) from chitosan. The absorption at 1080–1020 cm^{-1} was assigned to C–O–C stretching vibrations of the polysaccharide backbone and PVA's C–O stretching (Sanchez-García et al., 2008).

Upon amaaddition of roselle anthocyanins (b–f), the overall band positions were retained but with subtle intensity changes and slight shifts. Notably, the broad O–H/N–H band between 3300–3200 cm^{-1} became broader and more intense, suggesting increased hydrogen bonding between anthocyanin hydroxyl groups and the polymer matrix. Peaks near 1650 cm^{-1} and

© 2026 The Authors.

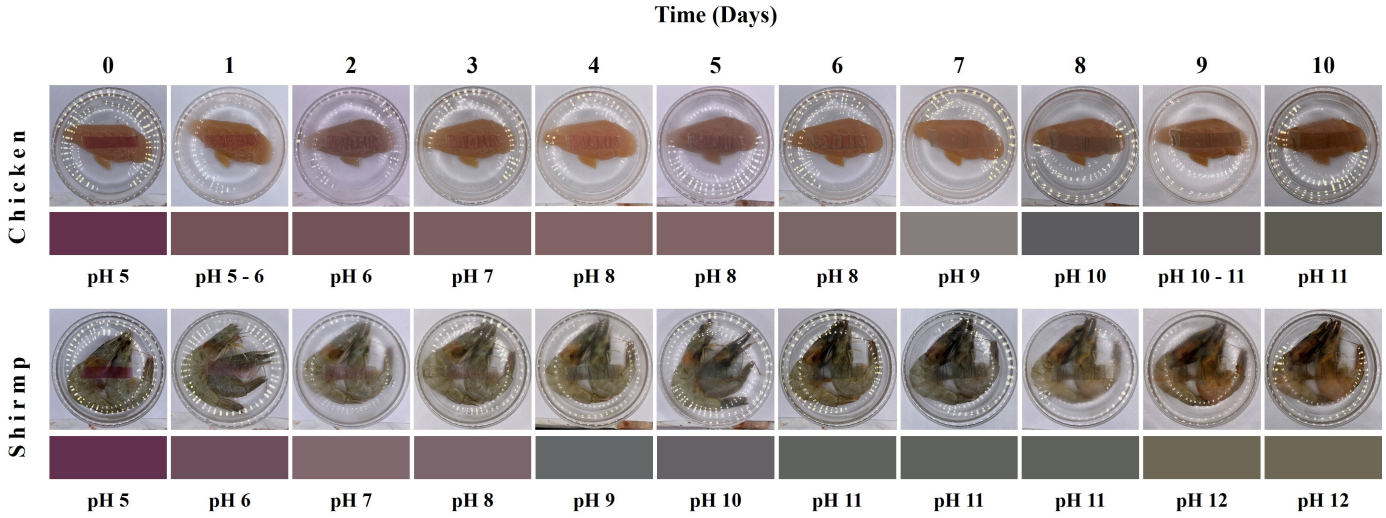

Figure 12. Evaluation of Chicken and Shrimp Meat Storage at Refrigeration Temperature (6 °C) Over Several Days

1540 cm^{-1} showed minor shifts to lower wavenumbers, indicating possible interactions between the anthocyanin's carbonyl groups and the amino/hydroxyl groups of chitosan and PVA (Amaregouda and Kamanna, 2023; Li and Li, 2025).

Furthermore, the appearance of weak shoulders in the 1400–1200 cm^{-1} region may be attributed to phenolic C–O stretching and aromatic C=C vibrations of anthocyanins incorporated into the film. These findings corroborate previous reports that embedding natural pigments such as anthocyanins into polysaccharide–PVA matrices produces new hydrogen-bonded networks without generating new covalent bonds, thereby preserving the integrity of the pigments while enhancing matrix compatibility (Amaregouda et al., 2023).

Overall, the FTIR spectra confirm successful incorporation of roselle anthocyanins into the Cs/PVA matrix, with evidence of intermolecular interactions, primarily hydrogen bonding, between the polymer functional groups and anthocyanin molecules. This interaction is essential for pigment stability within the film and can influence both mechanical and colorimetric performance in smart sensor applications.

3.2.5 Determination of Colorimetric Film Thickness

Film thickness is a critical parameter influencing the mechanical integrity, barrier properties, and optical response of colorimetric indicator films. As shown in Figure 8, the thickness of Cs/PVA–roselle anthocyanin films increased progressively with longer maceration durations, ranging from 119 ± 0.02 (μm) (R1) to 161 ± 0.01 (μm) (R5). This trend reflects the higher anthocyanin content incorporated into the polymer matrix from extended maceration, which increases the solid fraction and viscosity of the casting solution, ultimately producing thicker films upon solvent evaporation.

The observed thickness enhancement can be mechanistically attributed to stronger hydrogen bonding and hydrophobic interactions between anthocyanin chromophores and the hydroxyl/amino groups of chitosan and PVA. These interactions promote denser molecular packing and a more cohesive polymer network (Li and Li, 2025). Comparable effects have been reported in other bioactive-enriched films, where polyphenolic compounds strengthened the polymer matrix through hydrogen bonding interactions, leading to enhanced crosslinking density and mechanical stability (Amaregouda et al., 2023; Xu et al., 2023).

From a functional perspective, thicker films can improve pigment retention and barrier stability, thereby prolonging operational durability. However, excessive thickness may compromise transparency and slow down optical responsiveness, which is a critical parameter for real-time freshness monitoring (Li et al., 2019).

3.3 Colorimetric Behavior of Cs/PVA–Roselle Films under Ammonia Vapor Exposure

Table 1 shows the visual color response of pristine Cs/PVA and Cs/PVA–roselle anthocyanin (R1–R5) films under 1% ammonia vapor for up to 240 min. The pristine Cs/PVA film retained a neutral gray tone with negligible color shift, whereas the anthocyanin-loaded films exhibited a pronounced and time-dependent color transition from reddish-purple to yellowish-brown. This chromatic shift arises from the pH-dependent structural transformation of anthocyanins from the flavylium cation to their quinoidal base and chalcone forms under alkaline conditions, which is well documented in the literature (Cruz et al., 2022; Tang et al., 2019).

Increasing the maceration time (R1 → R5) progressively enriched the anthocyanin content within the Cs/PVA matrix. As a result, the initial color intensity became more vivid, and the rate of color change under ammonia exposure accelerated. Notably, Cs/PVA–R5 displayed the most distinct and stable color transition among all formulations. This finding suggests that extended maceration time leads to higher anthocyanin

© 2026 The Authors.

Table 2. Colorimetric Responses of the Cs/PVA–R5 Film at pH Values Ranging from 3.0 to 12.0, Expressed as CIELAB Coordinates and ΔE Values (n=3)

Treatment of Film	pH	(L* ± SD)	(a* ± SD)	(b* ± SD)	(ΔE ± SD)	Color of Film
Initial Color	–	31.23 ± 0.25^{a}	33.10 ± 0.10^{i}	-3.00 ± 0.10^{c}	–	
Final Color	3	34.97 ± 1.89^{b}	35.18 ± 1.33^{j}	-3.33 ± 0.11^{c}	4.57 ± 0.73^{a}	
	4	37.23 ± 0.39^{c}	31.61 ± 0.51^{h}	-1.30 ± 0.77^{d}	6.44 ± 0.63^{b}	
	5	39.82 ± 1.91^{d}	23.89 ± 1.03^{g}	-2.98 ± 0.19^{c}	12.62 ± 2.00^{c}	
	6	45.21 ± 0.30^{e}	21.35 ± 0.31^{f}	-7.24 ± 0.42^{a}	18.76 ± 0.22^{d}	
	7	51.39 ± 1.12^{g}	14.87 ± 0.80^{e}	-4.26 ± 0.64^{b}	27.21 ± 1.20^{e}	
	8	46.97 ± 0.75^{f}	8.65 ± 0.64^{d}	1.57 ± 0.46^{e}	29.44 ± 0.40^{f}	
	9	44.89 ± 0.52^{e}	2.55 ± 0.68^{c}	1.97 ± 0.48^{e}	33.83 ± 1.03^{g}	
	10	48.40 ± 0.40^{f}	1.18 ± 0.01^{b}	4.16 ± 0.03^{f}	36.95 ± 0.40^{h}	
	11	38.16 ± 0.06^{c}	-5.39 ± 0.29^{a}	7.17 ± 0.58^{g}	40.41 ± 0.31^{i}	
	12	60.23 ± 0.21^{h}	3.55 ± 0.01^{c}	14.84 ± 0.29^{h}	45.08 ± 0.08^{j}	

Note: The notation with different "letters" indicates a significant difference (p<0.05)

extraction and improved pH-responsive behavior in the resulting films, which is in agreement with previous findings on anthocyanin-enriched smart films (Amaregouda et al., 2023).

In this study, Cs/PVA–R5 can therefore be regarded as the optimal formulation, combining high pigment concentration with adequate film homogeneity to deliver the most reliable colorimetric response under alkaline vapors. Such behavior is consistent with earlier reports showing that increasing bioactive loading within biopolymer matrices enhances the responsiveness of pH-indicator films without compromising their structural integrity (Che Hamzah et al., 2022; Latiff et al., 2025).

Figure 9 presents the colorimetric sensitivity (%S) of pristine Cs/PVA and Cs/PVA–R1 to Cs/PVA–R5 films under 1% ammonia vapor for 240 min. The pristine Cs/PVA film exhibited negligible responsiveness (S% <5%), confirming the absence of pH-indicative chromophores. In contrast, the anthocyanin-loaded films displayed marked, time-dependent increases in sensitivity. Among these, Cs/PVA–R5 achieved the highest response (40%S) with the fastest rate of change within the first 60 min and stabilization between 120–180 min. This trend underscores R5 as the optimal formulation for achieving rapid and robust colorimetric detection of alkaline volatiles.

The observed performance enhancement with increasing maceration time can be attributed to higher anthocyanin and polyphenolic contents in the films. These bioactives enhance hydrogen bonding, π–π interactions, and electrostatic linkages with the hydroxyl and amino groups of the Cs/PVA matrix, facilitating faster ammonia diffusion to reactive sites and amplifying chromophoric transitions (Mu et al., 2025). Notably, Cs/PVA–R5 offers a balanced combination of high pigment loading, optimal film thickness, and uniform dispersion, resulting in superior colorimetric performance compared to other formulations.

This finding aligns with earlier reports on anthocyanin-based freshness indicators, where optimized pigment concentrations accelerate sensory response and improve real-time accuracy of food spoilage monitoring (Liu et al., 2022; Wang et al., 2022). Therefore, Cs/PVA–R5 can be recommended as the optimal composite film for real-time freshness indication in smart sensor systems.

3.4 Colorimetric Characteristics and pH Responsiveness of Film Formulations

Considering all physicochemical and optical attributes, the Cs/PVA–R5 formulation was selected as the most suitable candidate. This choice is justified by its more intense, saturated color, indicative of higher anthocyanin loading, which enhances its sensitivity to environmental changes. Consequently, Cs/PVA–R5 is expected to deliver the most pronounced and reliable color transitions upon exposure to volatile ammonia, a key spoilage marker, thereby offering superior performance in freshness sensing applications. This observation is in line with previous findings showing that increases in volatile nitrogenous compounds such as TVB-N correlate strongly with increasing ΔE values of colorimetric indicators. For instance, the TVB-N content of hairtail fish rose from 2.42 ± 0.02 mg/100 g to 21.10 ± 0.05 mg/100 g within 36 h, reaching 35.09 ± 1.64 mg/100 g at the end of storage, at which point corresponding colorimetric films displayed significantly elevated ΔE values (p < 0.05), confirming spoilage-driven chromatic transitions (Chen et al., 2021).

A progressive increase in lightness (L*) from 31.23 at the initial color to 60.23 at pH 12 indicated a gradual loss of color saturation and a more translucent appearance at higher pH. Simultaneously, the a* value (red–green axis) decreased sharply from +33.10 at the initial state to +3.55 at pH 12, reflecting a reduction in red chromaticity and the emergence of greenish or yellowish tones. Conversely, the b* value (yellow–blue axis) shifted from -3.00 to +14.84, indicating a strong shift toward the yellow region. These patterns are consistent with

© 2026 The Authors.

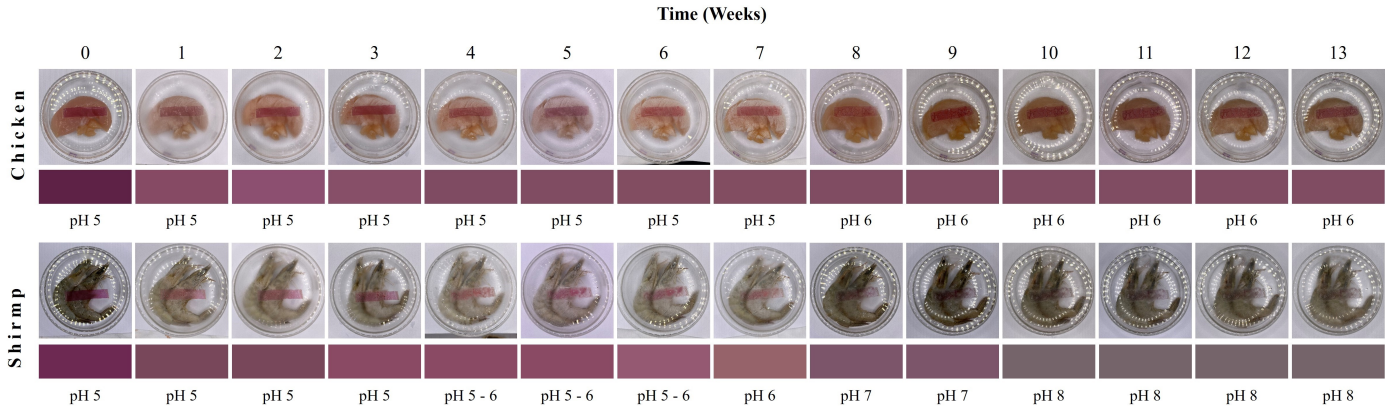

Figure 13. Evaluation of Chicken and Shrimp Meat Storage at Freezing Temperature (–10 °C) Over Several Weeks

the well-known multistate equilibrium of anthocyanins across pH environments, which modulates their optical properties.

The statistical analysis using one-way ANOVA ($p < 0.05$) revealed significant differences among the mean values of L*, a*, b*, and ΔE across the tested pH levels, as indicated by different superscript letters in Table 2. The lightness (L*) values increased markedly from 31.23 ± 0.25 at the initial state to 60.23 ± 0.21 at pH 12, demonstrating a progressive brightening of the film surface as the medium shifted from acidic to alkaline. Meanwhile, the a* coordinate, representing redness, decreased significantly from 33.10 ± 0.10 to 3.55 ± 0.01, confirming the loss of red hue as deprotonation occurred. The b* coordinate shifted from negative (–3.00 ± 0.10, indicating bluish tones) to positive (14.84 ± 0.29 at pH 12), showing the gradual emergence of yellow-green hues. These shifts collectively explain the sharp increase in total color difference (ΔE), which rose from 4.57 ± 0.73 at pH 3 to 45.08 ± 0.08 at pH 12, demonstrating high colorimetric sensitivity toward pH variation.

Statistical validation confirmed that the differences among treatments were highly significant ($p < 0.05$), verifying that each pH range produced distinct chromatic behavior. According to ISO 11664–4 standards, ΔE values above 5 are considered perceptible to the human eye, confirming that the Cs/PVA–R films achieved highly distinguishable color transitions across the tested pH range. The greatest chromatic contrast was observed between acidic (pH 3–4) and alkaline conditions (pH ≥ 10), which is particularly advantageous for freshness monitoring applications where amine volatilization drives local pH elevation. (Chen et al., 2025a).

Furthermore, the linear regression analysis between total color difference (ΔE) and pH for the Cs/PVA–R5 film demonstrates an exceptionally strong and statistically robust correlation (Figure 10) with an outstanding coefficient of determination R^2=0.996. This result indicates that 99.6% of the ΔE variation is explained by pH, and that each unit increase in pH yields an average rise of 4.4 ΔE units. The high linearity and narrow error distribution confirm the film's excellent sensitivity, reproducibility, and predictive capability across the full pH spectrum.

From a materials perspective, the incorporation of roselle anthocyanins into the Cs/PVA matrix provided a homogeneously distributed chromogenic system capable of rapid pH response. The hydrogen-bonding and electrostatic interactions between anthocyanins and chitosan–PVA likely stabilized the pigments and reduced leaching, while still permitting rapid protonation–deprotonation equilibria at the film surface (Nguyen et al., 2025). The resulting system combines high sensitivity with visual clarity, making it suitable for integration into biodegradable freshness indicators for perishable foods.

Collectively, these findings demonstrate that Cs/PVA–R films can act as effective visual pH indicators over a broad range (pH 3–12), with ΔE values surpassing typical thresholds for human visual detection. This performance underscores the films' potential for real-time monitoring of food spoilage, where the release of volatile amines from proteins causes measurable pH elevation and thus distinct color changes.

3.5 Mechanism of Color Transition in the Cs/PVA–R5 Film

The Cs/PVA–R5 film consists of a semi-interpenetrating polymer matrix of chitosan and poly(vinyl alcohol) (PVA) entrapping anthocyanins derived from roselle anthocyanin extract. In this hybrid system, anthocyanins act as the pH-responsive chromophore, while the chitosan–PVA network modulates molecular mobility, hydration dynamics, and proton transfer, thereby influencing the optical response.

As shown in Figure 11, under acidic conditions (pH 1–3), anthocyanins predominantly exist in the flavylium cation form, stabilized by the proton-rich environment as well as electrostatic interactions with protonated amino groups of chitosan. This structural configuration yields a distinct red to magenta coloration, which is uniformly distributed within the polymer matrix due to strong hydrogen bonding between anthocyanin hydroxyl groups and PVA's secondary hydroxyl moieties.

Upon exposure to slightly acidic to neutral conditions (pH

© 2026 The Authors.

4–7), partial hydration of the chromophore occurs, converting the flavylium cation into the carbinol pseudobase, a colorless or pale-pink species. This transformation is facilitated by the film's moderate water uptake and the plasticizing effect of PVA, which enhances anthocyanin accessibility to nucleophilic water molecules.

At moderately alkaline conditions (~ pH 8), deprotonation leads to formation of the quinonoidal base, which possesses extended conjugation and absorbs at longer wavelengths, yielding a purple to violet coloration. Here, the chitosan matrix plays a critical role: its decreasing protonation at rising pH increases the free volume of the polymer network, allowing greater resonance stabilization of the quinonoidal form.

Further deprotonation at pH 9–11 produces the anionic quinonoidal base, inducing a shift toward blue-green or greenish tones. The enhanced electron delocalization is stabilized by hydrogen bonding with both PVA and residual protonated domains of chitosan. At strongly alkaline conditions (≥ pH 12), irreversible ring-opening of the anthocyanin flavylium core yields chalcone derivatives, characterized by a yellowish coloration. This structural transition is supported by increased hydroxide ion accessibility as the polymer network becomes more relaxed and hydrophilic at high pH.

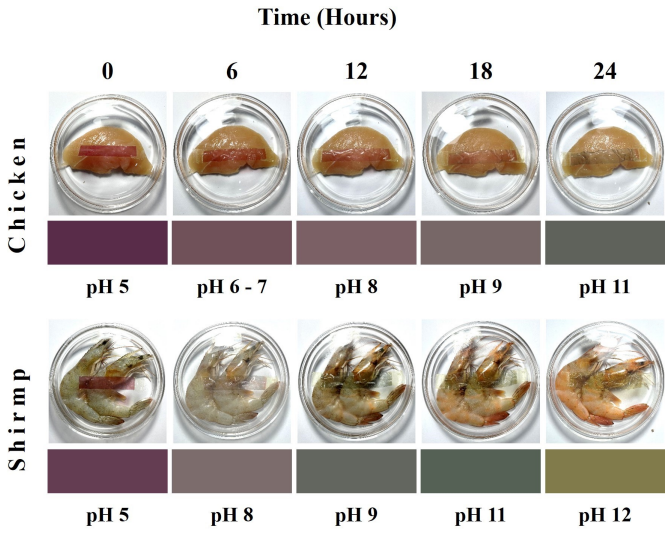

Figure 14. Evaluation of Chicken and Shrimp Meat Storage at Ambient Temperature (23 °C) Over Several Hours

3.6 Application of Colorimetric Films for Monitoring Chicken and Shrimp Freshness

3.6.1 Refrigeration Storage Conditions

Figure 12 presents the dynamic colorimetric responses of Cs/PVA–R5 film in contact with chicken and shrimp samples stored at 6 °C for ten days. At day 0, both chicken and shrimp exhibited an initial pH of 5.0, characteristic of fresh muscle tissue, which corresponded to the red–purple coloration of the films dominated by the flavylium cation form of anthocyanins. As storage progressed, microbial metabolism and endogenous enzymatic activity induced proteolysis and deamination reactions, leading to the accumulation of volatile basic nitrogenous compounds such as ammonia, trimethylamine (TMA), and dimethylamine (DMA). These catabolic processes resulted in a gradual rise in sample pH, reaching 8–9 for chicken and 11–12 for shrimp after 9–10 days, in line with advanced spoilage stages. Importantly, meat and seafood are generally considered unfit for consumption once their pH exceeds the threshold of 7.0–7.8, beyond which microbial spoilage becomes critical and safety is compromised (Karanth et al., 2023).

The spoilage threshold by referring to quantitative evidence reported in the literature. According to Wang et al. (2022), the pH of shrimp increased from approximately 6.3 in fresh samples to 7.7 after extended storage, correlating with a sharp rise in Total Volatile Basic Nitrogen (TVB-N) levels beyond 25 mg/100 g, which is widely recognized as the critical limit for seafood spoilage. Similarly, chicken meat samples exhibited pH increases from 6.0 to above 7.0, coinciding with microbial counts exceeding 8 log CFU/g and sensory signs of deterioration. The films' optical responses tracked these biochemical changes with high fidelity. At pH 5–6 (fresh state), the films maintained an intense red–purple coloration due to the prevalence of protonated flavylium ions. As the pH increased to 7–9 (intermediate spoilage), the films underwent a perceptible shift toward brownish–green, reflecting the dominance of quinoidal base species. In severely spoiled samples (pH ≥10), the chromatic profile shifted to yellow–brown, consistent with the formation of anthocyanin chalcone structures under alkaline conditions. These sequential and irreversible color transitions provide a direct visual proxy for the biochemical deterioration of meat and seafood matrices.

Overall, the strong correlation between pH elevation, volatile amine accumulation, and film color change validates the Cs/PVA–roselle anthocyanin system as a reliable and real-time freshness indicator for refrigerated chicken and shrimp. The tunable chromatic responses not only enable qualitative spoilage detection but also hold potential for semi-quantitative estimation of freshness based on distinct colorimetric thresholds.

3.6.2 Freezing Storage Conditions

Figure 13 shows the colorimetric responses and pH progression of chicken and shrimp during frozen storage (–10 °C) over 13 weeks. At week 0, both chicken and shrimp exhibited initial pH values of 5.0 with a reddish appearance in the indicator film, confirming their initial freshness. Throughout the first 4–5 weeks, only slight changes in pH were observed (chicken pH 5–6; shrimp pH 5–6), indicating that freezing substantially slowed down microbial metabolism and enzymatic activity compared with refrigerated storage. This stability is consistent with the well-established effect of low-temperature storage in suppressing spoilage reactions.

By weeks 8–10, a gradual pH increase became apparent in shrimp (pH 7–8) and to a lesser extent in chicken (pH 6), corresponding to the slow accumulation of volatile basic nitrogenous

© 2026 The Authors.

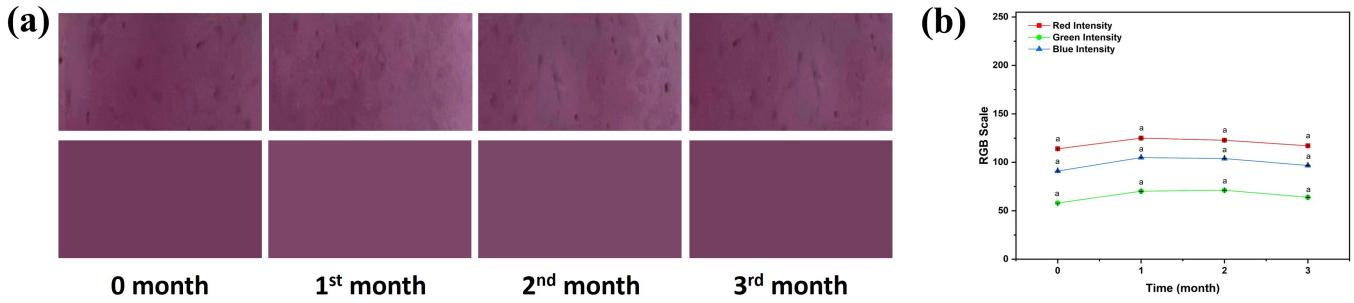

Figure 15. Long-Term Color Stability of the Cs/PVA–R5 Film During Three Months of Storage at Ambient Temperature. (a) Visual Appearance (top) and Corresponding RGB Intensity Values (Bottom). (b) Quantitative RGB Scale Analysis (n = 3). Bars or Data Points Annotated with the Same Letter are Not Significantly Different ($p < 0.05$)

compounds such as ammonia, trimethylamine (TMA), and dimethylamine (DMA). The indicator films responded to these changes by shifting from pink–purple hues toward brownish or gray tones, with ΔE values increasing proportionally to the rise in pH. These findings confirm that the Cs/PVA–roselle anthocyanin films retained their chromatic sensitivity under frozen conditions and were able to track spoilage-related changes in real time.

Interestingly, shrimp displayed a faster pH elevation than chicken, reaching pH 8 by week 12–13, while chicken remained near pH 6. This difference reflects shrimp's higher enzymatic activity and greater susceptibility to psychrotrophic microorganisms, even under freezing conditions. The indicator films captured this distinction clearly, demonstrating their potential for differentiating freshness dynamics among different protein matrices.

3.6.3 Ambient Temperature Conditions

Figure 14 illustrates the pH progression and visible color changes of chicken and shrimp monitored with Cs/PVA–roselle anthocyanin indicator films during ambient storage (23 °C) for 24 hours. At time zero, both chicken and shrimp maintained initial pH values near 5.0, with the indicator films showing a deep purplish hue characteristic of the anthocyanin flavylium form. After only 6 hours, chicken pH had risen to 6–7 and shrimp to pH 8, indicating the onset of microbial deamination and proteolysis that release volatile bases such as ammonia, trimethylamine (TMA), and dimethylamine (DMA).

By 12–18 hours, both samples exhibited pronounced increases in pH (chicken to pH 8–9, shrimp to pH 9–11), accompanied by a clear shift in the indicator film from reddish-purple toward brownish-green tones. This chromatic transition reflects the structural transformation of anthocyanins from the protonated flavylium cation to less colored quinoidal bases and chalcones under alkaline conditions. Such changes coincide with the known rapid spoilage of protein-rich foods at ambient temperatures, where microbial growth and enzymatic reactions accelerate markedly compared to chilled or frozen conditions.

By 24 hours, shrimp reached pH 12 and chicken pH 11, representing extensive spoilage. The indicator films displayed the strongest color contrast at this stage, underscoring their high sensitivity to volatile base accumulation. Shrimp consistently showed faster pH elevation than chicken, confirming its greater perishability due to higher free amino acid content and more active endogenous enzymes.

Among all result, the Cs/PVA–R5 film yielded the clear and consistent chromatic transitions during the 24-hours test. This is attributable to its higher anthocyanin loading, which increases available chromophoric sites and hydrogen-bonding interactions with the Cs/PVA matrix, thereby accelerating the sensor response and improving color stability under highly alkaline conditions. These results establish that Cs/PVA–roselle anthocyanin films function as reliable colorimetric indicators for monitoring the freshness of frozen poultry and seafood over extended storage periods. By combining visual cues with quantifiable CIELAB and ΔE metrics, the system offers a non-destructive, consumer-friendly, and environmentally sustainable approach for real-time cold-chain quality control.

3.7 Long-term Color Stability Evaluation of the Cs/PVA–R5 Film

The long-term color stability of the Cs/PVA–R5 colorimetric film was evaluated over a three-month storage period under freezing conditions (–10 ± 1 °C) with controlled low humidity. As shown in Figure 15a, the visual appearance and corresponding digital color representation of the film remained remarkably stable from the freshly prepared state (0 month) through the third month of storage. The film retained its characteristic purplish hue with no noticeable fading, discoloration, or phase separation, indicating that the anthocyanin pigments were well-preserved within the Cs/PVA polymer matrix.

This excellent visual stability can be attributed to strong intermolecular hydrogen bonding between the hydroxyl groups of PVA, the amino groups of chitosan, and the hydroxyl/carbonyl groups of the roselle anthocyanins. Such interactions effectively immobilize the pigment molecules within the biopolymer network, limiting molecular mobility and minimizing pigment oxidation or degradation over time (Chen et al., 2025b;

© 2026 The Authors.

Meng et al., 2024; Singh et al., 2021). Furthermore, the semicrystalline nature of PVA and the dense molecular packing of the Cs/PVA composite create a protective microenvironment that shields anthocyanins from exposure to oxygen, light, and moisture key factors responsible for pigment deterioration. In addition, the inherent antioxidant and antimicrobial properties of chitosan may further stabilize the anthocyanin molecules by reducing oxidative stress within the film matrix (Ding et al., 2024; Rais et al., 2025; Zhang et al., 2025).

To quantitatively validate the color stability, RGB analysis was performed on the Cs/PVA–R5 film throughout the three-month storage period (Figure 15b). The RGB intensity values for red, green, and blue channels showed only minimal variation, maintaining a consistent balance indicative of excellent color retention. The red channel intensity ranged from 120–130, the blue from 95–105, and the green from 60–70, reflecting the film's stable chromatic properties. Statistical analysis using one-way ANOVA ($p < 0.05$) revealed no significant differences ($p > 0.05$) among RGB values across the 0-, 1-, 2-, and 3-month storage intervals, as indicated by the same superscript letters in the plot. These findings confirm that the minor variations observed fall within experimental error. Standard deviations were calculated based on duplicate measurements ($n = 3$), further validating the reproducibility and precision of the data.

Overall, both visual and quantitative results demonstrate that the Cs/PVA–R5 film possesses outstanding long-term optical stability, retaining its visual integrity and chromatic balance for up to three months under normal storage conditions. This stability underscores the effectiveness of the chitosan–PVA hybrid matrix in protecting roselle anthocyanins from environmental degradation and highlights the film's potential as a durable, reliable, and shelf-stable colorimetric sensor for intelligent food freshness monitoring applications.

4. CONCLUSIONS

This study demonstrates that the Cs/PVA–R5 formulation exhibits the highest responsiveness and visual clarity among the tested anthocyanin-based indicators, driven by structural transformations of anthocyanins upon exposure to alkaline volatile amines. These results reinforce the feasibility of using pH-responsive anthocyanin matrices as low-cost and eco-friendly smart sensors for real-time freshness monitoring. Nevertheless, this work is limited by the absence of statistical correlations between colorimetric responses and quantitative spoilage indicators. The future work should establish stronger predictive reliability by statistically correlating colorimetric shifts with validated spoilage indices (e.g., TVB-N, microbial load), while also assessing stability, packaging integration, and consumer readability under real supply-chain conditions.

5. ACKNOWLEDGEMENT

This work was partly supported by the Ministry of Higher Education, Science and Technology through the Applied Research Grant (No. 657/UN10.A0501/B/PT.01.03.2/2025).

REFERENCES

Abdelghany, A., A. Menazea, and A. Ismail (2019). Synthesis, Characterization and Antimicrobial Activity of Chitosan/Polyvinyl Alcohol Blend Doped with *Hibiscus Sabdariffa* L. Extract. *Journal of Molecular Structure*, **1197**; 603–609

Amaregouda, Y. and K. Kamanna (2023). Preparation and Characterization of Indicator Films from Chitosan/Polyvinyl Alcohol Incorporated *Stachytarpheta jamaicensis* Anthocyanins for Monitoring Chicken Meat Freshness. *Sustainable Food Technology*, **1**; 738–749

Amaregouda, Y., K. Kamanna, and A. Kamath (2023). Multifunctional Bionanocomposite Films Based on Chitosan/Polyvinyl Alcohol with ZnO NPs and *Carissa carandas* Extract Anthocyanin for Smart Packaging Materials. *ACS Food Science & Technology*, **3**(9); 1411–1422

Augustyńska-Prejsnar, A., M. Kačániová, P. Hanus, Z. Sokołowicz, and M. Słowiński (2024). Microbial and Sensory Quality Changes in Broiler Chicken Breast Meat During Refrigerated Storage. *Foods*, **13**(24); 4063

Bi, S., J. Pang, L. Huang, M. Sun, X. Cheng, and X. Chen (2020). The Toughness Chitosan-PVA Double Network Hydrogel Based on Alkali Solution System and Hydrogen Bonding for Tissue Engineering Applications. *International Journal of Biological Macromolecules*, **146**; 99–109

Castañeda-Ovando, A., M. D. L. Pacheco-Hernández, M. E. Páez-Hernández, J. A. Rodríguez, and C. A. Galán-Vidal (2009). Chemical Studies of Anthocyanins: A Review. *Food Chemistry*, **113**(4); 859–871

Che Hamzah, N. H., N. Khairuddin, I. I. Muhamad, M. A. Hassan, Z. Ngaini, and S. R. Sarbini (2022). Characterisation and Colour Response of Smart Sago Starch–Based Packaging Films Incorporated with *Brassica oleracea* Anthocyanin. *Membranes*, **12**(9); 913

Chen, H., X. Dong, K. Ou, X. Cong, Y. Liao, Y. Yang, and H. Wang (2025a). A pH-Responsive Dual-Emission Composite for Fast Detection of BAs and Visual Monitoring Seafood Freshness with Large Luminescence Color Difference. *Talanta*, **282**; 126946

Chen, M., T. Yan, J. Huang, Y. Zhou, and Y. Hu (2021). Fabrication of Halochromic Smart Films by Immobilizing Red Cabbage Anthocyanins into Chitosan/oxidized-Chitin Nanocrystals Composites for Real-Time Hairtail and Shrimp Freshness Monitoring. *International Journal of Biological Macromolecules*, **179**; 90–100

Chen, X., H. Xiang, Y. Liang, J. He, R. Chen, Z. Zhu, S. Li, X. Chen, and S. Cheng (2025b). Highly Stable and Multifunctional Intelligent Film Based on Grape Skin Anthocyanin, Polyvinyl Alcohol, Chitosan and Selenopeptide: Preparation, Characterization and Application. *Food Hydrocolloids*, **158**; 110546

Cruz, L., N. Basílio, N. Mateus, V. De Freitas, and F. Pina (2022). Natural and Synthetic Flavylium-Based Dyes: The

© 2026 The Authors.

Chemistry Behind the Color. *Chemical Reviews*, **122**(1); 1416–1481

Ding, C., W. Ma, and J. Zhong (2024). The Influence of Microcrystalline Structure and Crystalline Size on Visible Light Transmission of Polyvinyl Alcohol Optical Films. *Optical Materials*, **147**; 114627

Du, J., H. Dai, H. Wang, Y. Yu, H. Zhu, Y. Fu, L. Ma, L. Peng, L. Li, Q. Wang, and Y. Zhang (2021). Preparation of High Thermal Stability Gelatin Emulsion and Its Application in 3D Printing. *Food Hydrocolloids*, **113**; 106536

Enaru, B., G. Drețcanu, T. D. Pop, A. Stănilă, and Z. Diaconeasa (2021). Anthocyanins: Factors Affecting Their Stability and Degradation. *Antioxidants*, **10**(12); 1967

Erna, K. H., W. X. L. Felicia, J. M. Vonnie, K. Rovina, K. W. Yin, and M. N. Nur'Aqilah (2022). Synthesis and Physicochemical Characterization of Polymer Film-Based Anthocyanin and Starch. *Biosensors*, **12**(4); 211

Fiddaroini, S., F. Prisilia, S. B. Karo, L. Madaniyah, A. D. Khairana, G. Rahmaniah, S. Amalia, Aulanni'am, M. F. Rahman, L. Dinira, Q. Fardiyah, and A. Sabarudin (2025). Green Synthesis of Nanoparticles Using Cottonwood and Rambutan Honeys: Optimization, Characterization, and Enhanced Antioxidant Activity with Reduced Toxicity Via Oligochitosan Coating. *Next Materials*, **8**; 100685

Genç, İ. Y., G. R, and A. E (2025). Quality Determination of Frozen-Thawed Shrimp Using Machine Learning Algorithms Powered by Explainable Artificial Intelligence. *Food Analytical Methods*, **18**(6); 935–945

Gomes, B. T., L. L. Rodrigues Borges, N. M. E. P. De Leon Da Costa, T. R. Arruda, A. R. C. Ribeiro, C. S. Marques, P. C. Stringheta, T. V. De Oliveira, and N. D. F. F. Soares (2024). Gelatin/polyvinyl Alcohol Films Incorporated with Different Blueberry Extracts As Potential Colorimetric Indicators to Detect Acidic and Basic Vapors. *Food Control*, **165**; 110648

Karanth, S., S. Feng, D. Patra, and A. K. Pradhan (2023). Linking Microbial Contamination to Food Spoilage and Food Waste: The Role of Smart Packaging, Spoilage Risk Assessments, and Date Labeling. *Frontiers in Microbiology*, **14**; 1198124

Katiyo, W., H. L. De Kock, R. Coorey, and E. M. Buys (2020). Sensory Implications of Chicken Meat Spoilage in Relation to Microbial and Physicochemical Characteristics during Refrigerated Storage. *LWT – Food Science and Technology*, **128**; 109468

Klaharn, K., D. Pichpol, T. Meeyam, T. Harintharanon, P. Lohaanukul, and V. Punyapornwithaya (2022). Bacterial Contamination of Chicken Meat in Slaughterhouses and the Associated Risk Factors: A Nationwide Study in Thailand. *PLOS ONE*, **17**(6); e0269416

Kusumawati, R., Syamdidi, A. H. D. Abdullah, R. C. Nissa, B. Firdiana, R. Handayani, I. Munifah, F. R. Dewi, J. Basmal, and S. Wibowo (2025). Physical Properties of Biodegradable Chitosan-Cassava Starch Based Bioplastic Film Mechanics. *Science and Technology Indonesia*, **10**(1); 191–200

Lai, Y., Y. Chiang, Y. Jhan, T. Song, and M. Cheng (2024). Extraction Effects on Roselle Functionalities: Antioxidant, Antiglycation, and Antibacterial Capacities. *Foods*, **13**(14); 2172

Latiff, N. F., N. F. Sulaiman, M. I. Shaik, N. J. Mohamad, W. M. Khairul, A. I. Daud, and N. M. Sarbon (2025). Halochromic Smart Film: A Gelatin-Based pH-Sensitive Film Embedded with Anthocyanin from Roselle (*Hibiscus sabdariffa*) Extracts for Potential Food Spoilage Indicator Application. *Journal of Food Science*, **90**; e70134

Li, L. and Q. Li (2025). Advancements in Chitosan–Anthocyanin Composite Films: Sustainable Food Preservation with Biodegradable Packaging. *Foods*, **14**(10); 1721

Li, X.-M., J. Zhu, Y. Pan, R. Meng, B. Zhang, and H.-Q. Chen (2019). Fabrication and Characterization of Pickering Emulsions Stabilized by Octenyl Succinic Anhydride-Modified Gliadin Nanoparticle. *Food Hydrocolloids*, **90**; 19–27

Liu, D., C. Zhang, Y. Pu, S. Chen, L. Liu, Z. Cui, and Y. Zhong (2022). Recent Advances in pH-Responsive Freshness Indicators Using Natural Food Colorants to Monitor Food Freshness. *Foods*, **11**(13); 1884

Low, J. T., N. I. S. M. Yusoff, N. Othman, T. Wong, and M. U. Wahit (2022). Silk Fibroin-Based Films in Food Packaging Applications: A Review. *Comprehensive Reviews in Food Science and Food Safety*, **21**; 2253–2273

Ma, Y., L. Wen, Y. Liu, P. Du, P. Hu, J. Cao, and W. Wang (2024). Chitosan-Enhanced pH-Sensitive Anthocyanin Indicator Film for the Accurate Monitoring of Mutton Freshness. *Polymers*, **16**(6); 849

Mafe, A. N., G. I. Edo, R. S. Makia, O. A. Joshua, P. O. Akpoghelie, T. S. Gaaz, A. N. Jikah, E. Yousif, E. F. Isoje, U. A. Igbuku, D. S. Ahmed, A. E. A. Essaghah, and H. Umar (2024). A Review on Food Spoilage Mechanisms, Food Borne Diseases and Commercial Aspects of Food Preservation and Processing. *Food Chemistry Advances*, **5**; 100852

Mawarno, B. A. S., A. S. Putri, and I. Fitriana (2024). Effect of Maceration Time on Color Intensity, Bioactive Compounds and Antioxidant Activity of Purple Corn Extract (*Zea mays* var. Black Aztec). *JITIPARI*, **9**(2); 181–188

Meng, F., X. Yan, F. N. Nkede, M. H. Wardak, T. T. Van, F. Tanaka, and F. Tanaka (2024). An Intelligent Chitosan/Polyvinyl Alcohol Film with Two Types of Anthocyanins for Improved Color Recognition Accuracy and Monitoring Fresh-Cut Pineapple Freshness. *Food Packaging and Shelf Life*, **46**; 101402

Merlusca, I. P., D. S. Matiut, G. Lisa, M. Silion, L. Grădinaru, S. Oprea, and I. M. Popa (2018). Preparation and Characterization of Chitosan–Poly(vinyl Alcohol)–Neomycin Sulfate Films. *Polymer Bulletin*, **75**(12); 3971–3986

Mu, L., J. Bi, H. Zhao, J. Li, H.-M. Hou, G.-L. Zhang, H. Hao, and L. Zhou (2025). Intelligent pH-Responsive Films Based on Natural Blueberry Anthocyanins: A Non-Destructive Monitoring System for the Freshness of Aquatic Products with Prospective Smartphone Compatibility. *Food Chemistry:*

© 2026 The Authors.

X, **28**; 102587

Nguyen, K. D., D. N. D. Phung, T. T. T. Nguyen, O. T. K. Le, T. N. M. Cao, T. T. C. Truong, N. T. T. Phan, and A. P. Le Thi (2025). Colorimetric Chitosan/Polyvinyl Alcohol Composite Membrane Incorporated with Anthocyanins as pH Indicator for Monitoring Fish Freshness. *Journal of Applied Polymer Science*, **142**; e56333

Rais, A., M. Mennani, A. Bahloul, C. El Idrissi El Hassani, Z. Azoubi, R. Khiari, M. Oumam, A. Abourriche, and Z. Kassab (2025). pH-Sensitive Biodegradable Nanocomposite Films Incorporating Chitosan and Red Cabbage Anthocyanins. *International Journal of Biological Macromolecules*, **321**; 146278

Rosalina, Y., E. Warsiki, A. M. Fauzi, and I. Sailah (2022). Study of Anthocyanin Extraction from Red Banana (*Musa sapientum* L. var *Rubra*) Waste and Characteristics of Light Effects. *Science and Technology Indonesia*, **7**(4); 522–529

Sanchez-García, M. D., E. Gimenez, and J. M. Lagarón (2008). Morphology and Barrier Properties of Solvent Cast Composites of Thermoplastic Biopolymers and Purified Cellulose Fibers. *Carbohydrate Polymers*, **71**(2); 235–244

Sigurðardóttir, A. R., H. I. Sveinsdóttir, N. Schultz, H. Einarsson, and M. Guḍjónsdóttir (2025). Multispectral Imaging As a Predictive Tool for Freshness of Whole Atlantic Cod: Compared with Sensory, Chemical and Microbiological Analysis. *Applied Food Research*, *5*; 101130

Sinela, A., N. Rawat, C. Mertz, N. Achir, H. Fulcrand, and M. Dornier (2017). Anthocyanins Degradation during Storage of *Hibiscus sabdariffa* Extract and Evolution of Its Degradation Products. *Food Chemistry*, **214**; 234–241

Singh, S., O. F. Nwabor, D. M. Syukri, and S. P. Voravuthikunchai (2021). Chitosan-Poly(vinyl Alcohol) Intelligent Films Fortified with Anthocyanins Isolated from *Clitoria ternatea* and *Carissa carandas* for Monitoring Beverage Freshness. *International Journal of Biological Macromolecules*, **182**; 1015–1025

Suzery, M., B. Nudin, D. Nurwahyu Bima, and B. Cahyono (2020). Effects of Temperature and Heating Time on Degradation and Antioxidant Activity of Anthocyanin from Roselle Petals (*Hibiscus sabdariffa* L.). *International Journal of Science, Technology & Management*, **1**(4); 288–238

Tang, B., Y. He, J. Liu, J. Zhang, J. Li, J. Zhou, Y. Ye, J. Wang, and X. Wang (2019). Kinetic Investigation into pH-Dependent Color of Anthocyanin and Its Sensing Performance. *Dyes and Pigments*, **170**; 107643

Wang, D., X. Wang, Z. Sun, F. Liu, and D. Wang (2022). A Fast-Response Visual Indicator Film Based on Polyvinyl Alcohol/Methylcellulose/Black Wolfberry Anthocyanin for Monitoring Chicken and Shrimp Freshness. *Food Packaging and Shelf Life*, **34**; 100939

Wang, S., J. Wang, S. Wang, and S. Wang (2017). Annealing Improves Paste Viscosity and Stability of Starch. *Food Hydrocolloids*, **62**; 203–211

Xu, H., Y. Shi, L. Gao, N. Shi, J. Yang, and R. Hao (2023). Preparation and Characterization of pH-Responsive Polyvinyl Alcohol/ Chitosan/Anthocyanin Films. *Food Science and Technology*, **43**; e98022

Zhai, X., J. Shi, X. Zou, S. Wang, C. Jiang, J. Zhang, X. Huang, W. Zhang, and M. Holmes (2017). Novel Colorimetric Films Based on Starch/Polyvinyl Alcohol Incorporated with Roselle Anthocyanins for Fish Freshness Monitoring. *Food Hydrocolloids*, **69**; 308–317

Zhang, J., X. Zou, X. Zhai, X. Huang, C. Jiang, and M. Holmes (2019). Preparation of an Intelligent pH Film Based on Biodegradable Polymers and Roselle Anthocyanins for Monitoring Pork Freshness. *Food Chemistry*, **272**; 306–312

Zhang, K., Z. Li, X. Huang, Y. Qin, J. Zhang, S. B. H. Hashim, H. Xu, R. Zhang, J. Shi, and X. Zou (2025). Pore-Structure-Tunable Carboxymethyl Cellulose/Polyvinyl Alcohol Aerogel Functionalized with Butterfly Pea Anthocyanin for Real-Time Visual Monitoring of Pork Freshness. *Journal of Food Composition and Analysis*, **148**; 108491

Zhang, W., A. Khan, P. Ezati, R. Priyadarshi, M. A. Sani, N. B. Rathod, G. Goksen, and J. W. Rhim (2024). Advances in Sustainable Food Packaging Applications of Chitosan/Polyvinyl Alcohol Blend Films. *Food Chemistry*, **443**; 138506

Zhang, Y., D. Peng, X. He, H. Zheng, J. Xiao, D. Xu, and N. Yang (2026). Blueberry Anthocyanins-Functionalized Hydrogel Labels for Smartphone-Assisted Real-Time Visual Freshness Monitoring of Perishable Proteins. *Talanta*, **297**; 128813

Zhao, L., Y. Liu, L. Zhao, and Y. Wang (2022). Anthocyanin-Based pH-Sensitive Smart Packaging Films for Monitoring Food Freshness. *Journal of Agriculture and Food Research*, **9**; 100340

Zheng, D., S. Cao, D. Li, Y. Wu, P. Duan, S. Liu, X. Li, X. Zhang, and Y. Chen (2024). Fabrication and Characterization of Chitosan/Anthocyanin Intelligent Packaging Film Fortified by Cellulose Nanocrystal for Shrimp Preservation and Visual Freshness Monitoring. *International Journal of Biological Macromolecules*, **264**; 130692

© 2026 The Authors.